

SPATIAL DISTRIBUTION OF ENERGETIC ELECTRONS  
IN THE GEOMAGNETIC TAIL

TAKASHI MURAYAMA



THE UNIVERSITY OF CHICAGO

THE ENRICO FERMI INSTITUTE FOR NUCLEAR STUDIES

GPO PRICE \$ \_\_\_\_\_

CFSTI PRICE(S) \$ \_\_\_\_\_

Hard copy (HC) 2.00

Microfiche (MF) 50

ff 653 July 65

FACILITY FORM 602	<b>N66 35775</b>	
	(ACCESSION NUMBER)	(THRU)
	<u>41</u>	<u>1</u>
	(PAGES)	(CODE)
<u>CR-77630</u>	<u>29</u>	
(NASA CR OR TMX OR AD NUMBER)	(CATEGORY)	

SPATIAL DISTRIBUTION OF ENERGETIC ELECTRONS  
IN THE GEOMAGNETIC TAIL \*

TAKASHI MURAYAMA<sup>†</sup>  
Enrico Fermi Institute for Nuclear Studies  
University of Chicago  
Chicago, Illinois 60637

Laboratory for Astrophysics and Space Research  
Preprint No. EFINS 66-64

June 1966

\* This research was supported in part by the National Aeronautics and Space Administration under Grant NsG 179-61, the U. S. Air Force Office of Scientific Research under Grant AF 49 (638) 1642, and by the Air Force Cambridge Research Laboratories under Contract AF 19 (628) 2473.

<sup>†</sup> On leave from the Department of Physics, Nagoya University, Nagoya, Japan.

SPATIAL DISTRIBUTION OF ENERGETIC ELECTRONS  
IN THE GEOMAGNETIC TAIL

TAKASHI MURAYAMA\*  
Enrico Fermi Institute for Nuclear Studies  
University of Chicago  
Chicago, Ill. 60637

ABSTRACT

N66-35775


Counting rates from a solid state detector in the experiment of Fan, Gloeckler and Simpson on the IMP-1 satellite have been analyzed to investigate the spatial distribution of electrons with energies  $> 30$  kev in the geomagnetic tail and in the magnetosheath region surrounding the tail out to  $\sim 30$  earth radii. The counting rates range from the background cosmic ray level ( $\sim 3 \text{ sec}^{-1}$ ) up to  $10^3 \text{ sec}^{-1}$  and have a positive correlation with the  $K_p$  geomagnetic field disturbance index.

A multiple correlation analysis was made to investigate the spatial distribution of the electrons, which leads to the following results: Within the tail, 1) the particle flux is a decreasing function of  $Z_n$ , the distance from the neutral sheet as determined by magnetic field observations on the same satellite by Ness, Scarce and Seek.  $Z_n$  is found to be a better parameter for describing the electron distribution than the distance from either the ecliptic plane or the geomagnetic equatorial plane; 2) the radial dependence of the electron flux reported earlier by Anderson is shown to be due mostly to the spurious correlation between the radial distance and  $Z_n$ ; 3) for a given constant  $Z_n$ , the flux is higher near the dawn-side magnetospheric boundary than near the center of the tail.

---

\* On leave from the Department of Physics, Nagoya University, Nagoya, Japan





In the magnetosheath beyond the boundary of the tail, the electron flux decreases only gradually with increasing distance from the solar magnetospheric equatorial plane. The implications of these observations are discussed mainly in connection with the origin of the energetic electrons in the tail.

*Author*

## INTRODUCTION

Knowledge of geomagnetically trapped particles has been extended considerably beyond the well known Van Allen region up to about  $30 R_e$  (earth radii) by recent satellite experiments (Anderson et al., 1965; Anderson, 1965; Frank, 1965; Montgomery et al., 1965; Serlemitsos, 1966; Fan et al., 1966a; Konradi, 1966; Bame et al., 1966). It has also been possible to discuss their relation to the geomagnetic field since an extensive survey of the geomagnetic field on the IMP-I satellite made its tail-like configuration clear (Ness et al., 1964; Ness, 1965).

There is special interest in the high energy particles ( $> 30$  kev) observed in the tail of the geomagnetic field. It is found (Anderson, 1965) that they characteristically occur as isolated patches with a very short (a few minutes or less) buildup time for their flux and much slower decay. This fact suggests that they are accelerated locally or injected from outside into the tail in an impulsive manner. Particles in these events are mostly electrons, whose fluxes are highly fluctuating from background level up to  $10^7 \text{ cm}^{-2} \text{ sec}^{-1}$  above 45 kev (Anderson, 1965), associated with protons of much lower fluxes above 125 kev (Konradi, 1966). The energy spectra of the electrons can be approximated by a power law with indices ranging from 2.5 to 4.5 in an energy interval from 20 kev to 200 kev (Montgomery et al., 1965; Konradi, 1965). The measurement of the spectra was extended down to 0.2 kev by Bame et al. (1966).

Some of the results on the spatial distribution of these events also have been reported:

- (a) They appear to cluster about the geomagnetic equatorial plane and not the ecliptic plane (Montgomery et al., 1965).
- (b) There are no clear indications that they preferentially occur near the geomagnetic

neutral sheet (Anderson, 1965).

(c) The frequency of appearance of these fluxes has a radial dependence that rapidly falls off with increasing distance from the earth's center (Anderson, 1965).

(d) At a constant distance ( $18 R_e$ ) from the earth, they show a strong dawn-to-dusk asymmetry. They occur mainly in the range of local time from 20 hr. to 6 hr. (Montgomery et al., 1965).

These results are, however, not sufficient to study the origin of these events, for which precise knowledge of the spatial distribution has great importance. The difficulty of the analysis of their spatial distribution lies in the fact that many quantities which describe the position of the detector may possibly be related to the particle distribution. For instance, the geomagnetic coordinates and the solar ecliptic coordinates should be at least partially related to the spatial distribution because the geomagnetic field is responsible for the trapping of particles, while the solar wind makes the geomagnetic tail parallel to the ecliptic plane. In this sense, Ness (1965) proposed a new coordinate system called 'solar magnetospheric'<sup>\*</sup> in which the X-axis coincides with the sun-earth line and the XZ-plane involves the dipole vector of the earth. He showed that the geomagnetic neutral sheet in the tail agrees fairly well with the XY-plane of sm-coordinates. These coordinates are interdependent on one another in a complicated manner through the trajectory of the satellite. Therefore, special attention should be paid to the comparison of the effectiveness of these coordinates for describing the spatial distribution.

---

\* The word 'solar magnetospheric' will be abbreviated as 'sm', and similarly 'solar ecliptic' as 'se' and 'geomagnetic' as 'gm', respectively hereafter.

The purpose of this paper is to make a detailed study of the spatial distribution of energetic electrons in the tail, and to find out the most effective coordinate system to describe the spatial distribution. For this purpose, a multiple correlation analysis was made between the counting rate of an electron detector on board the IMP-I satellite and parameters which can possibly be related to the spatial distribution. As a result, we find that the distance from the neutral sheet of the geomagnetic tail has great importance for the spatial distribution. Namely, most of the energetic electrons are found to be concentrated within a few earth radii of the neutral sheet. The analysis also reveals a dawn-dusk asymmetry for the occurrence of the energetic electrons in the tail, but no significant importance of the geocentric distance is found for the spatial distribution. The energetic electrons in the magnetosheath region (defined as the region between the magnetospheric boundary and the bow shock) were also studied. The spatial distribution of the electrons in the region is appreciably different from that in the tail. However, no discontinuity of the electron intensity appears to exist at the magnetospheric boundary near the solar magnetospheric equatorial plane.

These results provide several important suggestions on the configuration of the geomagnetic tail and on the origin of the energetic electrons in the tail, which will be discussed in the last part of the paper.

#### DESCRIPTION OF THE EXPERIMENT

IMP-I was launched on November 27, 1963 into a highly eccentric orbit with a geocentric apogee distance of about  $31.5 R_e$  ( $\equiv$  earth radii), and an orbital period of about 3.9 days. The apogee-earth vector for the first orbit was  $25^\circ$

west of the sun-earth line, and due to the heliocentric motion of the earth, the subsequent apogee-earth vectors proceeded approximately  $4^\circ$  per orbit to the west of the sun. On the thirty-first orbit, which began on March 22, and beyond, the satellite remained inside the earth's magnetosphere at all times (Ness, 1965).

The data analyzed here were obtained by the front detector (called  $D_1$ ) of the cosmic ray telescope on board IMP-I, which has already been described (Fan et al., 1965; 1966a). Since the response of the  $D_1$  detector to energetic electrons has also been described in detail (Fan et al., 1966a), only a few of its main characteristics will be pointed out here.

- (a)  $D_1$  is a gold-silicon surface barrier detector with a surface area of  $3.5 \text{ cm}^2$  and a depletion depth of 200 microns.
- (b) Electrons of energy higher than 160 kev are in general counted individually by the detector system. The efficiency rises from zero at 160 kev to 0.6 at 270 kev and gradually declines to  $\sim 0.2$  at higher energies.
- (c) The detector is not sensitive to electrons of energy lower than 30 kev because of the aluminized mylar foil of  $1.5 \text{ mg/cm}^2$  thickness mounted on the surface of  $D_1$ .
- (d) At electron energies between 30 kev and 160 kev, detection results if two or more electrons 'pile up' in the detector within the resolving time of the system.
- (e) Translation of the  $D_1$  counting rate to the electron flux is not simple but depends on the electron energy spectrum. Only  $D_1$  counting rates will appear in the following sections.



## CHARACTERISTICS OF THE SPATIAL DISTRIBUTION OF ELECTRONS IN THE GEOMAGNETIC TAIL

As described before, orbit 31 of the IMP-I trajectory is the first orbit which lies completely in the magnetosphere. Figure 1 shows averaged  $D_1$  counting rates ( $I_{D1}$ ) over  $\sim 55$  minute intervals as a function of the universal time for this orbit. Beyond the trapped particle region, the rate changes rapidly with time ranging from background cosmic rates ( $\sim 3 \text{ sec}^{-1}$ ) up to  $10^3 \text{ sec}^{-1}$ . It is also clear from this figure that the variation has a component with a period of one day and a maximum at around 12 hr. This diurnal variation can be interpreted as an effect of the daily motion of the tilted geomagnetic dipole axis due to the earth's rotation. In fact, as shown in figure 1, the distance of our detector from the geomagnetic equatorial plane,  $Z_{gm}$ , shows a clear daily change. Also plotted in the figure is a quantity  $Z_{sm}$ , the distance from the solar magnetospheric equatorial plane, which has a trend similar to  $Z_{gm}$ . On the other hand, the change of  $Z_{se}$ , the distance from the ecliptic plane, has an almost monotonic nature showing that the se-coordinate is not adequate to account for the observed change of  $D_1$  rates. Furthermore, careful examination of figure 1 shows us that the phases of the daily changes of  $Z_{gm}$  and  $Z_{sm}$  are different from each other and  $Z_{sm}$  fits better with  $I_{D1}$  than  $Z_{gm}$ , at least qualitatively. All of these arguments are applicable to another example (orbit 35) shown in figure 2. These two figures strongly suggest that high energy electron events preferentially occur near the sm-equatorial plane, or near the geomagnetic neutral sheet taking account of the fact that the neutral sheet lies approximately on the sm-equatorial plane as reported by Ness (1965).

Figure 3 shows the results in orbit 40. A substantial part of this orbit lies near the center of the geomagnetic tail in contrast to orbits 31 and 35 which lie closer to the magnetospheric boundary. The daily change of  $I_{D1}$  is still recognizable in this figure, but unlike the preceding two, the change of  $Z_{sm}$  has a small diurnal component and the maxima of  $I_{D1}$  fit rather better to those of  $Z_{gm}$ . We interpret this change of behavior of  $D_1$  rates as follows. A good correspondence of  $Z_{sm}$  to  $I_{D1}$  in figures 1 and 2 suggests that the preferential occurrence of electron events near the neutral sheet. Measurements show, however, that the neutral sheet does not lie exactly on the  $sm$ -equatorial plane, especially at a long distance from the earth in the center of the tail. As already pointed out by Ness (1965), this deviation can be attributed to a spatial curvature of the neutral sheet in the periods when the geomagnetic dipole vector deviates appreciably from the  $Z_{sm}$  axis. As shown schematically in figure 4, the deviation of the sheet from the  $sm$ -equatorial plane ( $\Delta$ ) must be larger with increasing  $\chi$ , the geomagnetic latitude of the subsolar point. Although the precise estimate of  $\Delta$  as a function of  $\chi$  is difficult, we approximate this by the following:

$$\Delta = R_o \sin \chi \quad (1)$$

$R_o$  is a constant independent of the distance from the center of the earth, and may be determined by comparison with the measurements. In spite of the oversimplified form of (1), values of  $\Delta$  deduced from this equation with  $R_o = 8R_e$  is in satisfactory agreement with those obtained from the measurements (Behannon and Ness, 1965) shown in Table 1.

Table 1. Comparison of observed and calculated height of the neutral sheet from the solar magnetospheric equatorial plane.

orbit of IMP-I	observed height	calculated height
40	0.6 R <sub>e</sub>	1.6 R <sub>e</sub>
41	1.7 R <sub>e</sub>	2.0 R <sub>e</sub>
43	1.7	2.0
44	2.6	2.8
44	3.8	3.9

Thus we define a new parameter  $Z_n$  indicating the distance from the neutral sheet as follows

$$Z_n = \begin{cases} Z_{sm} & ( |Y_{sm}| > Y_o ) & (2a) \\ Z_{sm} - R_o \sin \chi & ( |Y_{sm}| < Y_o ) & (2b) \end{cases}$$

where the values  $Y_o = 8 R_e$  and  $R_o = 8 R_e$  are assumed in the following analysis.

Recent detailed study by the IMP-I magnetometer experiment of the location of the neutral sheet (Speiser, private communication) shows that these values are correct within an error of about 30 percent. The change of values within this range hardly affects the results in the following sections.

With the definition of  $Z_n$  shown above, the argument for the preferential occurrence of energetic electron events near the neutral sheet can be effective even in the central region of the tail.

## QUANTITATIVE TREATMENT OF THE SPATIAL DISTRIBUTION OF ELECTRON FLUXES IN THE TAIL

In view of the interdependence of one parameter with another, depending upon the position of the detector, examination of the simple relation between the electron flux and one parameter, such as geocentric distance, geomagnetic latitude, etc. may lead to a false conclusion. In order to avoid this effect, multiple correlation analyses, taking a few parameters at the same time, were done to confirm the arguments described in the preceding section.

### 1. Quantities in the correlation analysis

(a) Electron counting rate:  $J$

The quantity  $J$ , defined as follows, is used in the analysis:

$$J = \log_{10} I_e = \log_{10} (I_{D1} - I_{cr}) \quad (3)$$

where  $I_{cr}$  is a counting rate due to background cosmic rays. Three-hour averaged values of  $D_1$  rates were used in (3). Since our detector gives us no direct information on the fraction of  $I_{cr}$  in  $I_{D1}$ ,  $I_{cr}$  was estimated in the following way. The equation  $I_{D1} = I_{cr}$  holds if the detector is in interplanetary space at the time when no solar particles are expected to be incident on the detector. Figure 5 shows the  $D_1$  counting rates in the period of such a condition plotted versus Climax neutron monitor counting rates ( $I_N$ ) at corresponding periods. We can relate  $I_{cr}$  and  $I_N$  by the following equation.

$$I_{cr} = aI_N^2 + bI_N + c \quad (4)$$

constants  $a$ ,  $b$ , and  $c$  are determined by the least squares fit of (4) to the data.

Deviations of points from the curve thus obtained are sufficiently small so that the error of  $I_{cr}$  deduced from (4) is less than  $0.1 \text{ sec}^{-1}$  in the entire period of the IMP-I experiment.

(b) Geomagnetic activity index: K

Planetary magnetic indices  $K_p$ , given in three hour intervals, are used as one of the factors to be related to the electron counting rates.

(c) Radial distance: R

R is the distance of the detector from the center of the earth.

(d) Z values:  $Z_{sm}$ ,  $Z_{gm}$  and  $Z_n$

Three types of Z values are used, definitions of which have already been described and are briefly summarized below.

$Z_{sm}$ : Distance from the solar magnetospheric equatorial plane

$Z_{gm}$ : " from the geomagnetic equatorial plane

$Z_n$ : " from the neutral sheet

(e) Y value:  $Y_{sm}$

Distance from the X-Z plane of the solar magnetospheric coordinates is used as the third independent variable of the position of the detector.  $Y_{sm}$  is taken positive for the dusk side of the magnetosphere.

R, Z and Y values are given in units of earth radii.

## 2. Data in the tail region

Reliable data from our detector are available in the period from orbit 1 (November 1963) to orbit 43 (May 1964). In these orbits, portions of the satellite trajectory which lie in the magnetosphere are known from the results of magnetometer

measurements on the satellite (Ness, 1965). From the data in the period after the satellite was completely enclosed within the magnetosphere (orbits 31-43), some parts were omitted for the reasons described below.

(a) Solar protons of  $\sim 1 - 20$  Mev from a 27-day recurrent region were observed by the detector during several rotations (Fan et al., 1966b). Since the counts due to these particles are inseparable from those of electrons, and since physical conditions in the vicinity of the earth in such periods are probably different from those in undisturbed periods, data in orbits 31, 32, 37 and 38 which correspond to disturbed periods were excluded.

(b) A radiation region of relatively high and steady intensity is reported to exist at low geomagnetic latitude on the dark side of the earth, which sometimes extends to a distance of  $14 R_e$  (Anderson, 1965). Hence, the data at distances smaller than  $15 R_e$  were rejected.

As a result, 225 J values were obtained from orbits 33-36 (March 30 - April 14, 1964) and from orbits 39 - 43 (April 23 - May 11, 1964). (See figure 6.)

### 3. Results of multiple correlation analyses in the tail

First, we take three types of correlation J-K-R-Z<sub>gm</sub>, J-K-R-Z<sub>sm</sub> and J-K-R-Z<sub>n</sub> to compare the validities of different Z values. The analysis gives us two kinds of information:

(a) Partial correlation coefficients ( $r_{jk \cdot rz}$  etc.)

$r_{jk \cdot rz}$ , for example, means the correlation coefficient between J and K, with R and Z kept constant.

(b) Regression coefficients (  $\alpha$  ,  $\beta$  and  $\gamma$  )

These three values define a three dimensional plane as the best fit to the data points in the four dimensional space whose coordinate axes represent the four quantities in the analysis. The plane is described by the following equation.

$$J = \alpha K + \beta R + \gamma Z \quad (5)$$

in which J, K, R and Z values are normalized so that the mean value of each is zero. Numerical values of coefficients are listed in table 2.

Table 2. Coefficients of the multiple correlation of J-K-R-Z in the tail

type of Z	partial correlation coefficients			regression coefficients		
	$r_{jk \cdot rz}$	$r_{jr \cdot kz}$	$r_{jz \cdot kr}$	$\alpha$	$\beta$	$\gamma$
$Z_{gm}$	0.43	-0.05	-0.55	0.28	-0.010	-0.14
$Z_{sm}$	0.43	-0.21	-0.48	0.29	-0.041	-0.17
$Z_n$	0.50	-0.16	-0.63	0.30	-0.028	-0.22

In the table we see:

- (a) Correlations between J and Z are highly significant for any type of Z.  $Z_n$  gives the highest value although not significantly higher than others.
- (b) The correlation between J and K is also sufficiently high to be in qualitative agreement with the result by Anderson (1965).
- (c) The correlation between J and R is lower than any of those referred to above and statistically insignificant.

The third result should be discussed in more detail because this contradicts a statement by Anderson (1965), namely, that the frequency of appearance

of electron events has a radial dependence which rapidly falls off with increasing geocentric distance. The origin of the discrepancy is estimated by the following fact: If only the data on inbound orbits are used, in the same manner as Anderson's treatment, and if the simple correlation is examined between J and R, these two quantities show significant correlation with a correlation coefficient of -0.50, much higher than any of  $r_{jr \cdot kz}$  in table 2. The result comes from a very high interdependence of Z and R in inbound orbits of IMP-I ( $r_{rZ} \sim 0.55$ ), which can transfer the correlation between J and Z to the one between J and R, or vice versa. Thus, a substantial part of the apparent radial dependence of the probability of occurrence of electron events can be explained by their Z dependence.

In the second step, we assume that no radial dependence of the electron flux exists and make corrections of all J values for the change of Kp index by using the coefficient obtained in table 2, and introduce  $J_k$  as calculated by the following equation.

$$J_k = J - \alpha K \quad (6)$$

Then, a simple correlation analysis is applied between Z and  $J_k$ , separately in each orbit. One example is shown in figure 7. Figure 8 shows a comparison between the correlation coefficients for  $Z_n$  and those for  $Z_{gm}$ . In eight out of nine orbits, coefficients for  $Z_n$  are higher than those for  $Z_{gm}$  and the difference between the averaged values of coefficients over nine orbits (-0.79 for  $Z_n$  and -0.63 for  $Z_{gm}$ ) is proved to be statistically significant with more than 99.9% confidence. Hence, we choose  $Z_n$  as the best parameter to describe the spatial distribution of electrons in the tail.



Figure 9 shows regression lines obtained by the procedure described above. We notice in the figure that the line is lower with increasing orbit number, keeping its slope nearly constant for the  $J_k - Z_n$  case, while for  $J - Z_{gm}$  it is not clear that this is the case. We regard this as a dependence of the electron flux on distance from the sun-earth line to the dawn-dusk direction. For the purpose of quantitative verification of this hypothesis, a multiple correlation analysis was again made after substituting  $Y_{sm}$  in the place of R in (5).

$$J = \alpha K + \delta Y_{sm} + \gamma Z \quad (7)$$

The results are shown in table 3.

Table 3. Coefficients of the multiple correlation of  $J-K-Y_{sm}-Z$  in the tail

type of Z	partial correlation coefficients			regression coefficients		
	$r_{jk.yz}$	$r_{jy.kz}$	$r_{jz.ky}$	$\alpha$	$\delta$	$\gamma$
$Z_n$	0.54	-0.49	-0.69	0.30	-0.063	-0.22

The correlation between J and  $Y_{sm}$  is sufficiently large to be statistically significant, and other coefficients are larger than those in table 2, although the difference is not significant.

We adopt the result of multiple correlation analysis among J, K,  $Y_{sm}$  and  $Z_n$  as the one which gives the highest correlation coefficients. Regression coefficients in this case give the following equation for the electron distribution in the tail region.

$$J_c = \log_{10} I_e = 0.30K - 0.063 Y_{sm} - 0.22 Z_n \quad (8a)$$

or

$$I_e \propto 10^{+(K/3.5)} 10^{-(Z_n/4.5)} 10^{-(Y_{sm}/16)} \quad (8b)$$

Effectiveness of equation (8) for describing the electron distribution can be evaluated by examining the difference between the observed values ( $J$ ) and the expected values given by equation 8a ( $J_c$ ). The rms difference of  $J - J_c$  is about 0.6, which means that the equation can predict the electron flux with an error of about a factor 4 at a given position in the tail and for a given Kp index at the corresponding time.

In figure 10,  $J$  and  $J - J_c$  are plotted against radial distance. Points in outbound orbits (black circles) and inbound orbits (open circles), rather separated from each other in the  $J$ - $R$  diagram, are well mixed in the  $(J - J_c)$ - $R$  diagram. In the latter, we still recognize a small correlation of points with  $R$ . The correlation coefficient is -0.22 and is significant in the statistical sense. However, this is not regarded as a proof of the existence of the radial dependence of electron fluxes, because the value depends strongly on the assumed form of dependence of  $J$  on any of the quantities  $K$ ,  $Z_n$  and  $Y_{sm}$ .

#### 4. Results for the magnetosheath region

The procedure used in the tail region was applied to data in the magnetosheath region. Three hour averaged counting rates in orbits 14-28 were picked up from the parts of the trajectory which lie in the magnetosheath region on the night side in local time (see figure 6). Data from orbits 17, 24, 29 and 30 were omitted since they were affected by particles from the solar flare event

of March 16, 1964 or the 27-day recurrent region.

Table 4 shows the results from 155 data points based on (5) in the magnetosheath region.

Table 4. Coefficients of the multiple correlation of J-K-R-Z in the magnetosheath region

type of Z	partial correlation coefficients			regression coefficients		
	$r_{jk \cdot rs}$	$r_{jr \cdot kz}$	$r_{jz \cdot kr}$	$\alpha$	$\beta$	$\gamma$
$Z_{gm}$	0.49	0.10	-0.29	0.24	0.016	-0.047
$Z_{sm}$	0.55	0.18	-0.44	0.27	0.028	-0.077

Here we see that the dependence of electron rates on the  $K_p$  index is similar to that in the tail. Correlation with  $Z_{sm}$  is significant but the regression coefficient

$\gamma$  is closer to zero than that in the tail and shows that electrons are far less concentrated about the solar magnetospheric equatorial plane than in the tail.

### DISCUSSION

In the preceding section, we have examined the statistical significance of correlations between the electron flux and various parameters, which may be related to the electron flux spatial distribution, assuming simple forms for their relationships as shown in (5) and (7). Figure 11 gives a more direct view of the spatial distribution, in which  $J_k$  values defined by (6) are classified into eight groups according to their magnitude and plotted against positions projected on the plane normal to the sun-earth line.

This figure naturally reflects the results obtained in the preceding section. High flux points are mainly clustered near the  $Y_{sm}$  axis, while low flux points are usually far from the axis but closer to the left side of the figure

suggesting the dawn-dusk asymmetry. There is special interest in the continuity of the electron fluxes at the magnetospheric boundary near the  $Y$  axis. Although an insufficient number of points near the axis in the magnetosheath region does not allow us a distinct conclusion, there seems to be no clear discontinuity at the boundary.

In summary, we emphasize that reliable answers on the spatial distribution of energetic electrons in the tail may be obtained only through a multiple correlation analysis. The main conclusions deduced from the present multiple correlation analysis are as follows:

- (a) Energetic electron counting rates increase with increasing  $K_p$  index, both in the tail and in the magnetosphere.
- (b) The  $K_p$  dependence of the counting rates in both regions are quantitatively similar to each other.
- (c) The counting rates in the tail depend strongly on  $Z_n$ , the distance from the neutral sheet, so that most of the electrons are confined within a few earth radii from that sheet.
- (d) There is no significant dependence of the counting rates on geocentric distance.
- (e) The counting rates have a dawn-dusk asymmetry in the tail, those on the dawn side of the magnetosphere being higher than on the dusk side.
- (f) The dependence of the counting rates on  $Z_{sm}$ , the distance from the solar magnetospheric equatorial plane, in the magnetosheath region is much weaker than the  $Z_n$  dependence in the tail. But the dependence is still significant, showing the concentration, to some extent, of electrons toward the s-m equatorial plane.

(g) There is no clear discontinuity of the electron counting rates near the intersection of the neutral sheet and the dawn side boundary of the tail.

As discussed earlier, the result (d) is contrary to that reported by Anderson (1965), and leaves the question of radial dependence of the energetic electrons still open. Our result does not rule out the possibility of finding energetic electrons far beyond  $30 R_e$  in the tail, which relates to the problem concerning the length of the geomagnetic tail (Dessler, 1966).

The result (g) is important in connection with the problem of the origin of energetic electrons in the tail, because it suggests that electrons can flow into the tail via the neutral sheet as pointed out by Jokipii (1965). He also discussed the diffusion and convection of electrons found near the day side portion of the bow shock (Fan et al., 1966a) along the magnetosheath, and suggested that such electrons flowing down with the solar wind plasma could supply the electrons found in the tail. This model is consistent with the fact that the electrons are concentrated near the neutral sheet. It is also probable that these electrons are subject to an additional acceleration near the neutral sheet (for instance, by the mechanism proposed by Speiser (1965)).

The alternative possibility is that the origin of the electrons is in the magnetosphere: i.e., either the direct acceleration in the neutral sheet or a supply from the particle trapping region by such a mechanism as proposed by Ness and Williams (1966). Both of them satisfy the condition (c) of strong concentration of electrons near the neutral sheet.

In any case, the flux of energetic electrons confined near the

neutral sheet can be sufficiently high to 'flow out' to the magnetosheath region and be responsible for the concentration of electrons in the s-m equatorial plane in the magnetosheath region.

Finally we emphasize the dawn-dusk asymmetry (e), which supports a similar result already reported (Montgomery et al., 1965), as an important factor to investigate the origin of energetic electrons in the tail, although the satisfactory answer to this fact has not yet been given.

#### ACKNOWLEDGMENTS

The author wishes to express his hearty thanks to Prof. J. A. Simpson who enabled him to make the present analysis and gave him valuable advice during the work. He is also grateful to Dr. C. Y. Fan and Dr. J. R. Jokipii for their helpful discussions. The research was supported in part by the National Aeronautics and Space Administration under Grant NsG 179-61, the U. S. Air Force Office of Scientific Research under grant AF 49 (638) 1642, and the Air Force Cambridge Research Laboratories under contract AF 19 (628) 2473.

REFERENCES

- Anderson, K. A., H. K. Harris, and R. J. Paoli, Energetic electron fluxes in and beyond the earth's outer magnetosphere, *J. Geophys. Res.* 70, 1039-1050, 1965.
- Anderson, K. A., Energetic electron fluxes in the tail of the geomagnetic field, *J. Geophys. Res.* 70, 4741-4763, 1965.
- Bame, S. J., J. R. Asbridge, H. E. Felthouser, R. A. Olson, and I. B. Strong, Electrons in the plasma sheet of the earth's magnetic tail, *Phys. Rev. Letters* 16, 138-142, 1966.
- Behannon, K. W., and N. F. Ness, Magnetic storms in the earth's magnetic tail, *J. Geophys. Res.* 71, 2327-2351, 1966.
- Dessler, A. J., Discussion of letter by J. A. Van Allen, "Further remarks on the absence of a very extended magnetospheric tail", *J. Geophys. Res.*, 71, 2408-2410, 1966.
- Fan, C. Y., G. Gloeckler and J. A. Simpson, Cosmic radiation helium spectrum below 90 mev per nucleon measured on the IMP-1 satellite, *J. Geophys. Res.* 70, 3515-3527, 1965.
- Fan, C. Y., G. Gloeckler and J. A. Simpson, Acceleration of electrons near the earth's bow shock and beyond, *J. Geophys. Res.* 71, 1837-1856, 1966a.
- Fan, C. Y., G. Gloeckler and J. A. Simpson, Protons and helium nuclei within interplanetary magnetic regions which co-rotate with the sun, *Proc. Ninth Int. Conf. Cosmic Rays, London, Vol. 1*, 109-111, The Physical Society, 1966b.
- Frank, L. A., A survey of electrons  $E > 40$  kev beyond 5 earth radii with Explorer 14, *J. Geophys. Res.* 70, 1593-1626, 1965.

- Jokipii, J. R., Diffusion and convection of energetic electrons behind the earth's bow shock, Enrico Fermi Inst. Rept., EFINS-65-93, University of Chicago, 1965.
- Konradi, A., Electron and proton fluxes in the tail of the magnetosphere, J. Geophys. Res. 71, 2317-2325, 1966.
- Montgomery, M. D., S. Singer, J. P. Conner, and E. E. Stogsdill, Spatial distribution, energy spectra, and time variation of energetic electrons ( $E > 50$  kev) at 17.7 earth radii, Phys. Rev. Letters 14, 209-213, 1965.
- Ness, N. F., The earth's magnetic tail, J. Geophys. Res. 70, 2989-3005, 1965.
- Ness, N. F., C. S. Scarce and J. B. Seek, Initial results of the IMP-I magnetic field experiment, J. Geophys. Res. 69, 3531-3569, 1964.
- Ness, N. F., and D. J. Williams, Correlated magnetic tail and radiation belt observations, J. Geophys. Res. 71, 322-325, 1966.
- Serlemitsos, P., Low-energy electrons in the dark magnetosphere, J. Geophys. Res. 71, 61-77, 1966.
- Speiser, T. W., Acceleration of particles in the neutral sheet of the geomagnetic tail, Proc. Ninth Int. Conf. Cosmic Rays, London, Vol. 1, 147-150, The Physical Society, 1966.



FIGURE CAPTIONS

- Fig. 1. Counting rates of the  $D_1$  detector measured on orbit 31 of IMP-I. Contributions to these rates come from electrons ( $> 30$  kev) of variable flux and cosmic rays ( $\sim 3 \text{ sec}^{-1}$ ). Distances from the solar ecliptic, the geomagnetic and the solar magnetospheric equatorial planes ( $Z_{se}$ ,  $Z_{gm}$  and  $Z_{sm}$ , respectively) are also shown.
- Fig. 2. Counting rates of the  $D_1$  detector for orbit 35 of IMP-I. (See figure 1 caption.)
- Fig. 3. Counting rates of the  $D_1$  detector for orbit 40 of IMP-I. (See figure 1 caption.) Distance from the neutral sheet,  $Z_n$  (defined by equation (2) in the text) is also shown.
- Fig. 4. Illustration of the deviation of the neutral sheet from the solar magnetospheric equatorial plane in the periods of high  $\chi$  ( $\equiv$  geomagnetic latitude of the subsolar point) values.
- Fig. 5. Correlation of the  $D_1$  counting rates on IMP-I in interplanetary space (November 1963 - February 1964) with Climax neutron monitor counting rates. The best fit curve for the form of equation (5) and the estimated uncertainty of the extrapolation of the curve are also shown.
- Fig. 6. Shaded areas show the regions projected on the ecliptic plane from which the data used in the quantitative analysis described in the text were taken.
- Fig. 7. Correlation diagrams of  $J_k - Z_{gm}$  and  $J_k - Z_n$  for orbit 35.

Fig. 8. Comparison of the correlation coefficients of two types of correlations  $J_k - Z_{gm}$  and  $J_k - Z_n$  for each orbit. The number attached to each point is the orbit number.

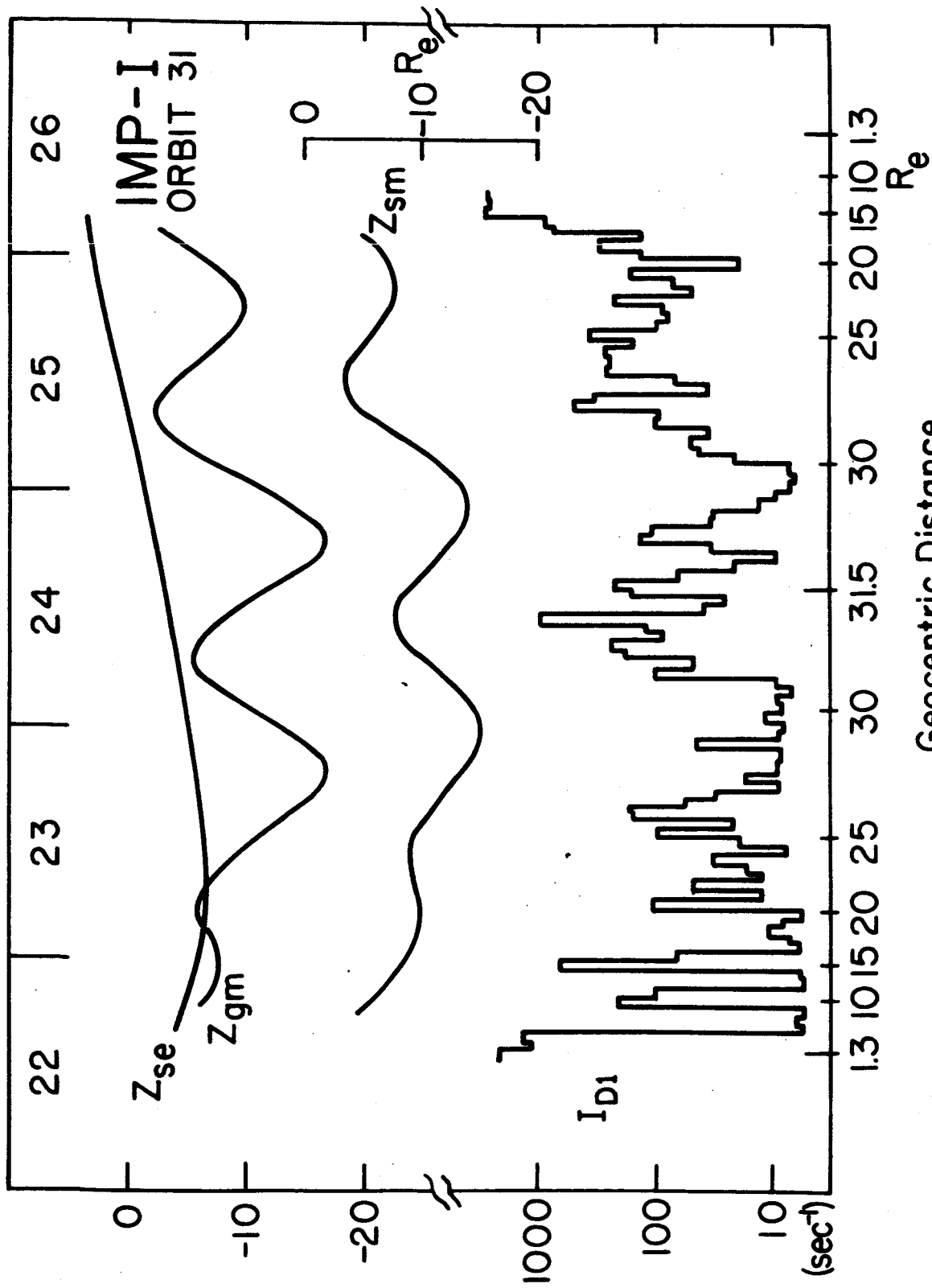
Fig. 9. Comparison of regression lines of different orbits obtained from correlation analyses of  $J_k - Z_{gm}$  and  $J_k - Z_n$ . Numbers attached to lines are orbit numbers.

Fig. 10. (a) Three hour averaged values of counting rates ( $I_e$ ) in the geomagnetic tail are plotted against the distance from the center of the earth.

(b) Differences between observed J values ( $J = \log I_e$ ) and those calculated from equation(9a) are plotted against the distance from the center of the earth.

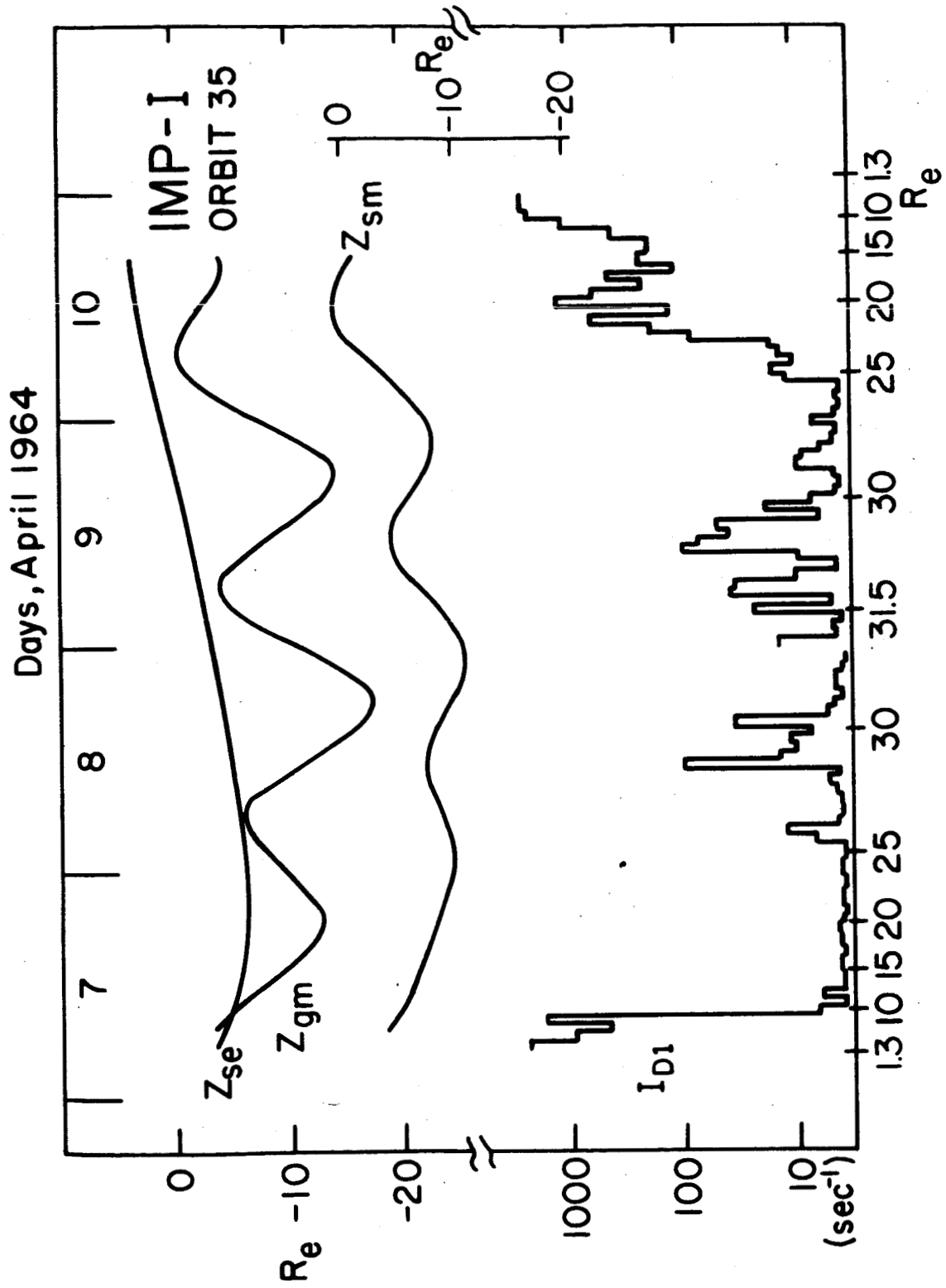
Fig. 11. Distribution of electron counting rates ( $> 30$  kev) in the tail region and in the magnetosheath region projected to the YZ plane of the solar magnetospheric coordinates. Two regions are separated by a dotted line. In the tail region,  $Z_n$ , defined by equation (2) in the text, is used instead of  $Z_{sm}$ , so that the ordinate shows the distance from the neutral sheet. The counting rates are corrected for the change due to their  $K_p$  dependence and normalized at  $K_p = 2$ .

Days, March 1964



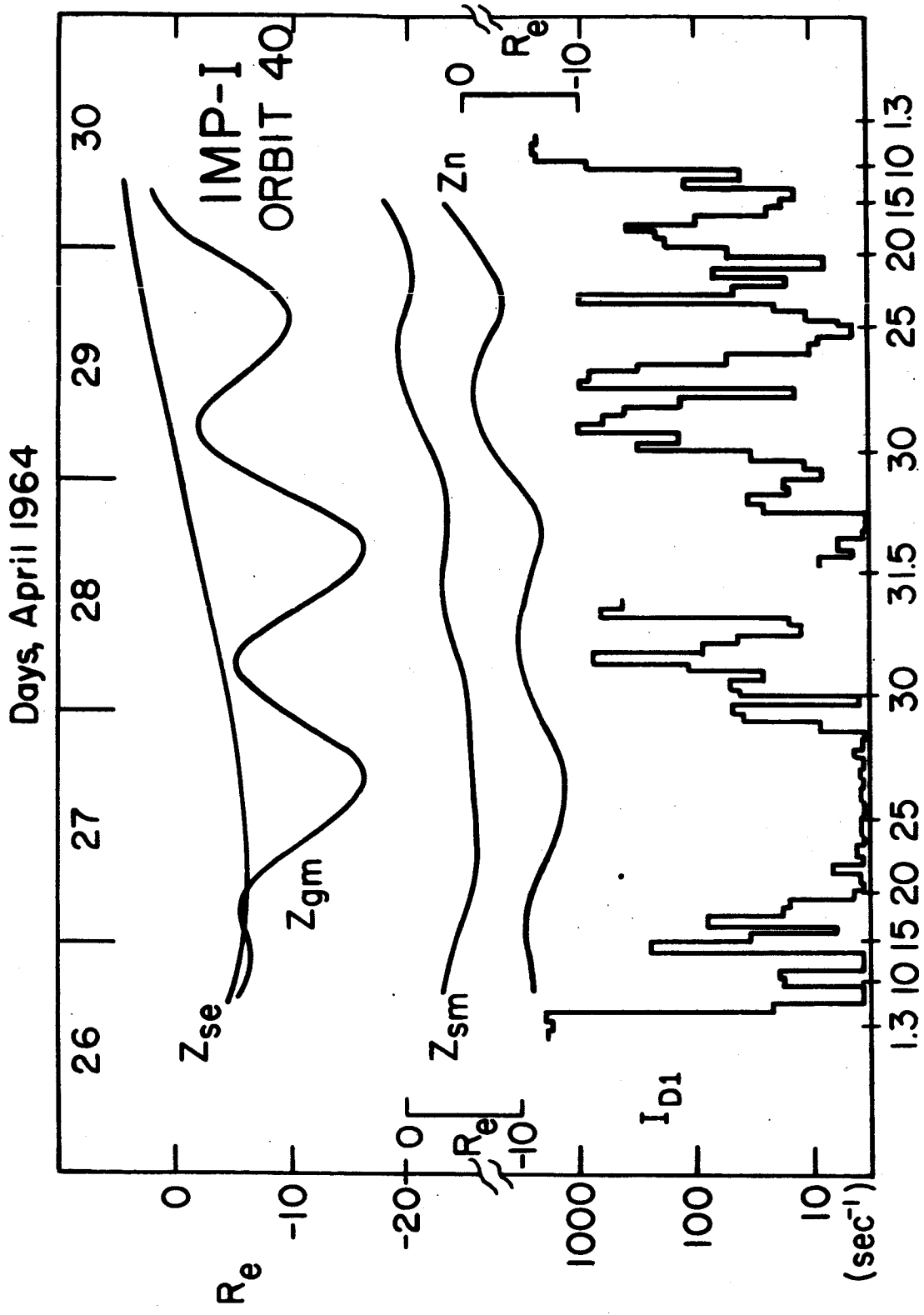
Geocentric Distance

Fig. 1



Geocentric Distance

Fig. 2



Geocentric Distance

Fig. 3

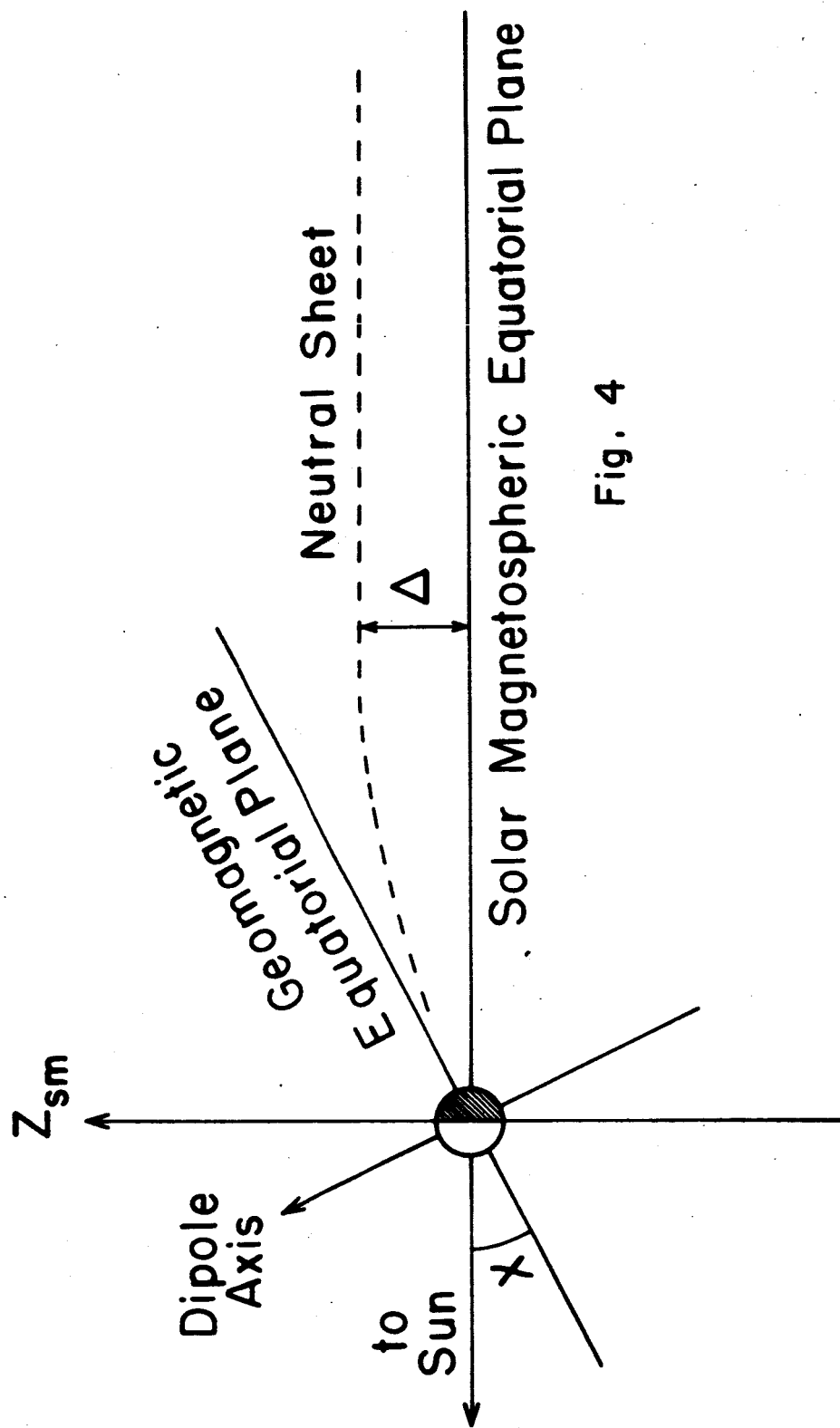
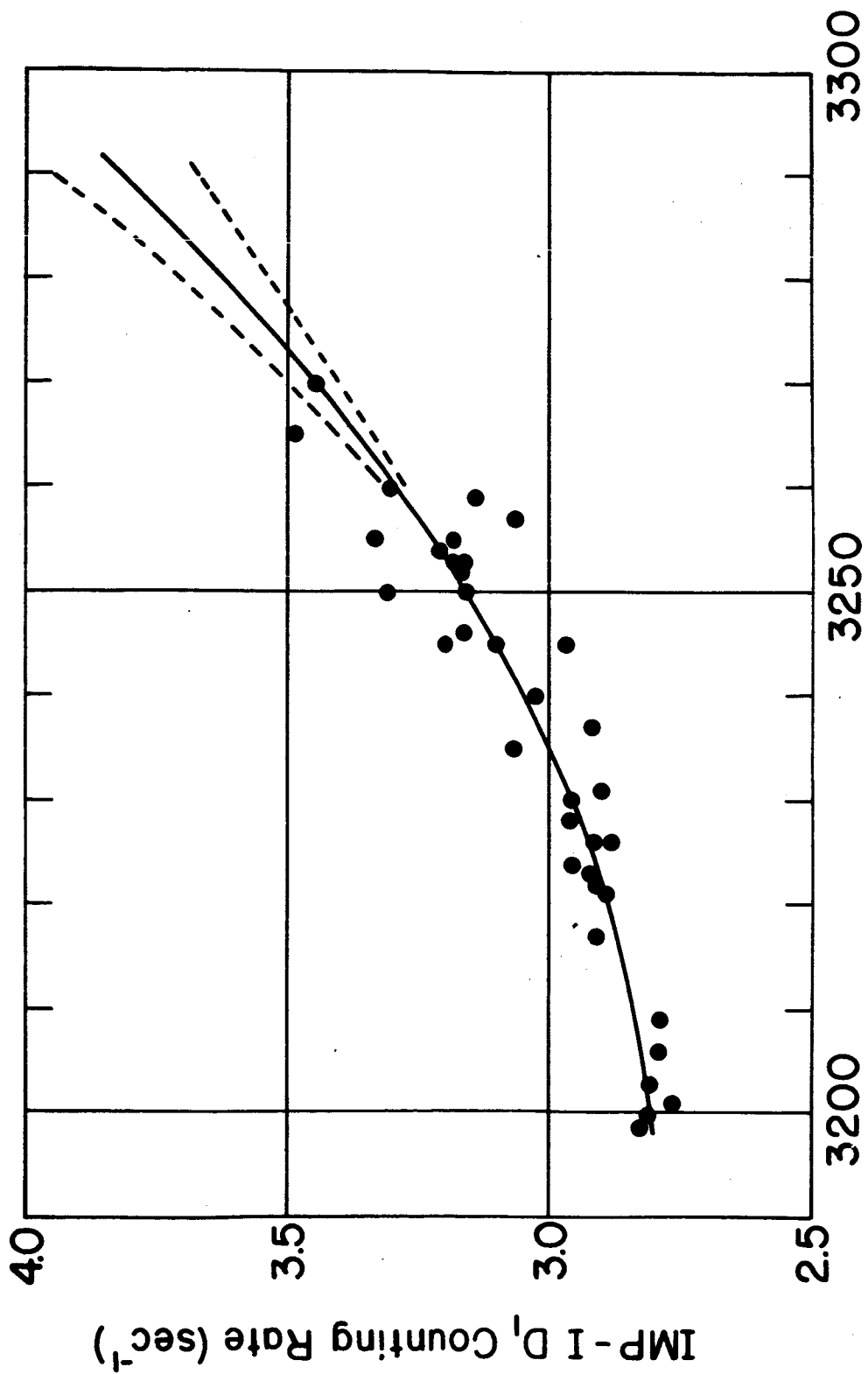


Fig. 4



Climax Neutron Monitor Counting Rate

Fig. 5

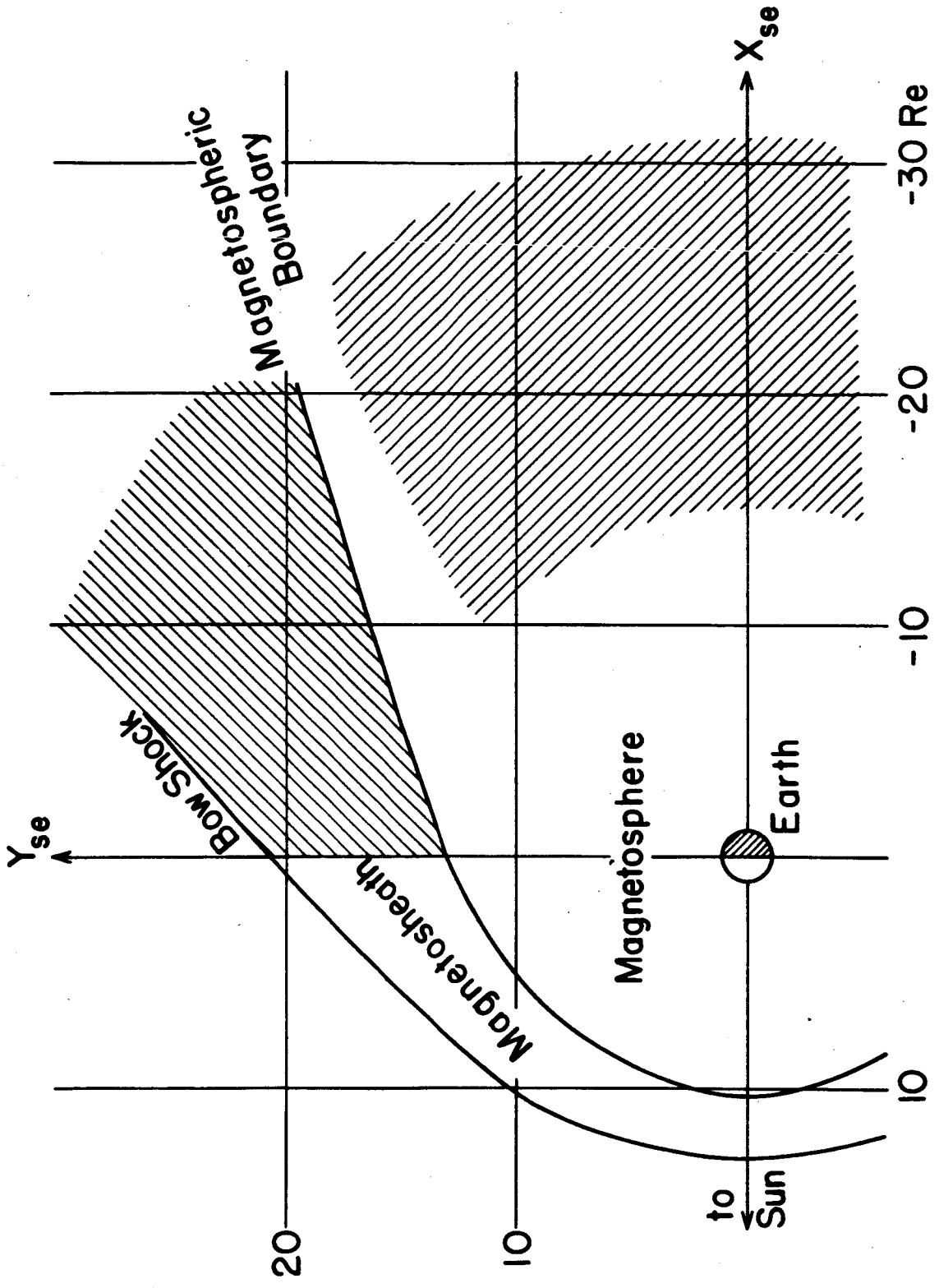


Fig. 6



Orbit 35

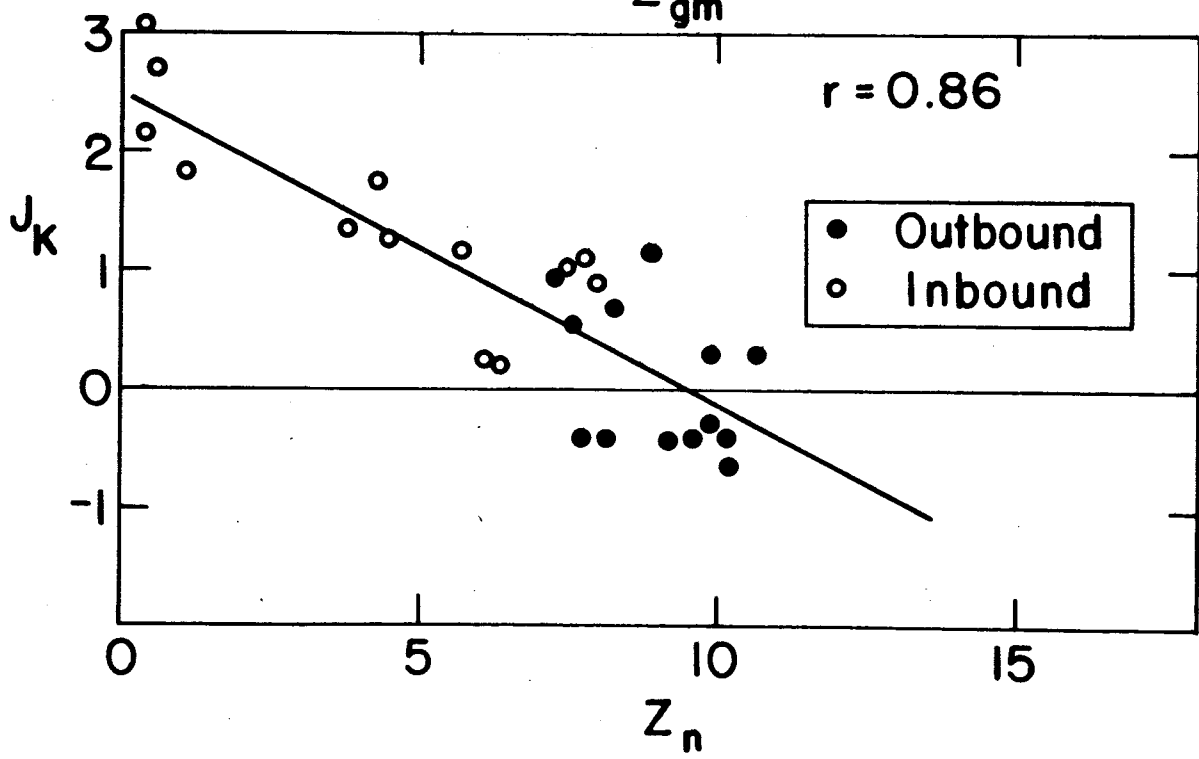
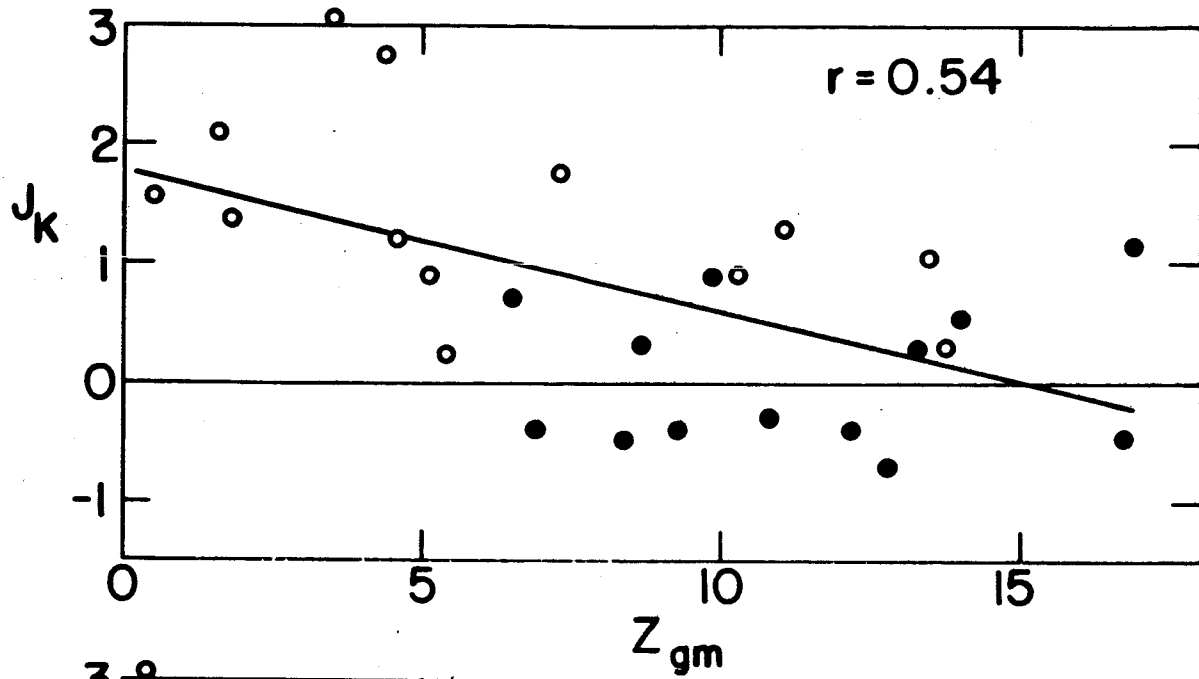


Fig. 7

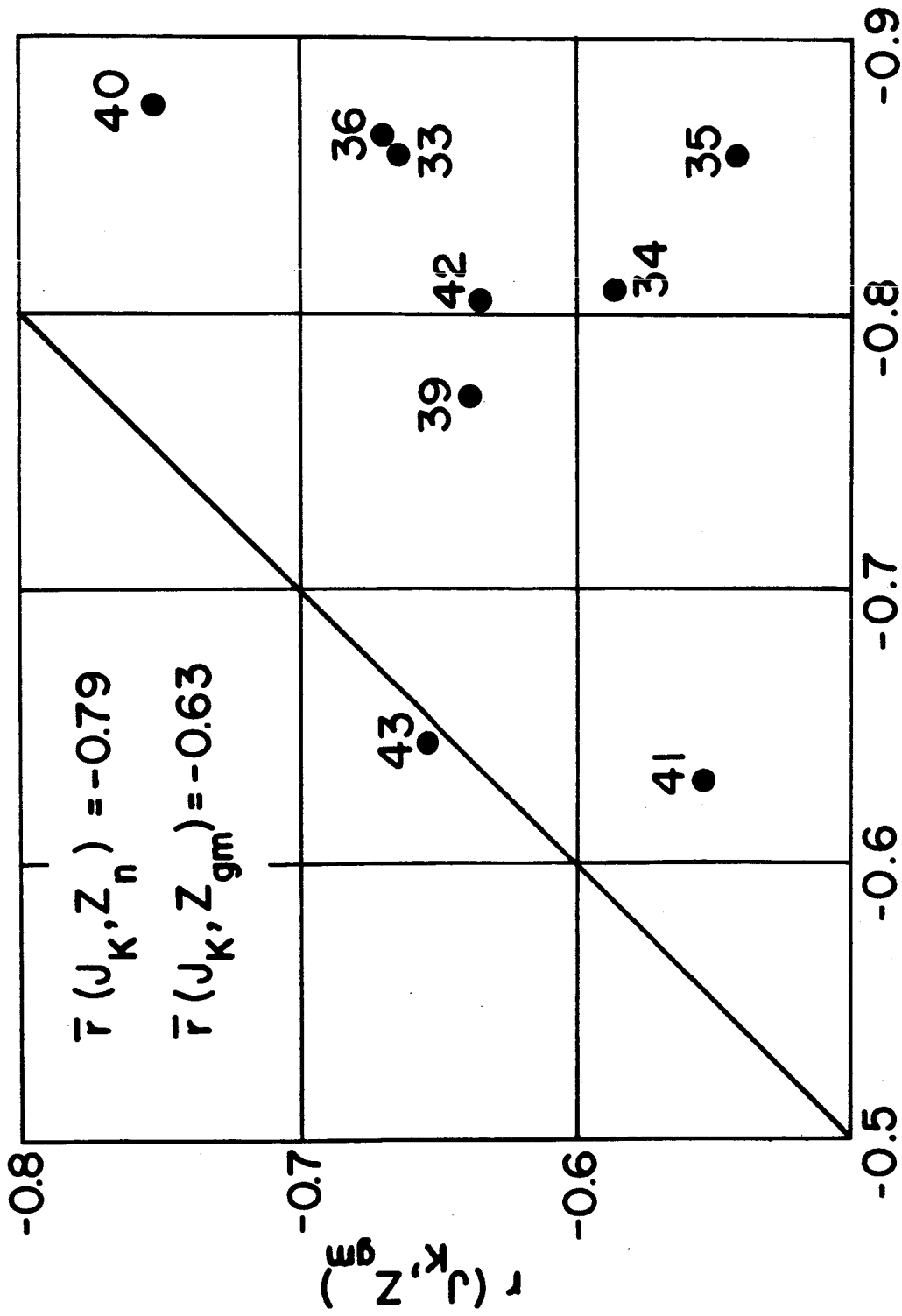


Fig. 8  $r(J_K, Z_n)$

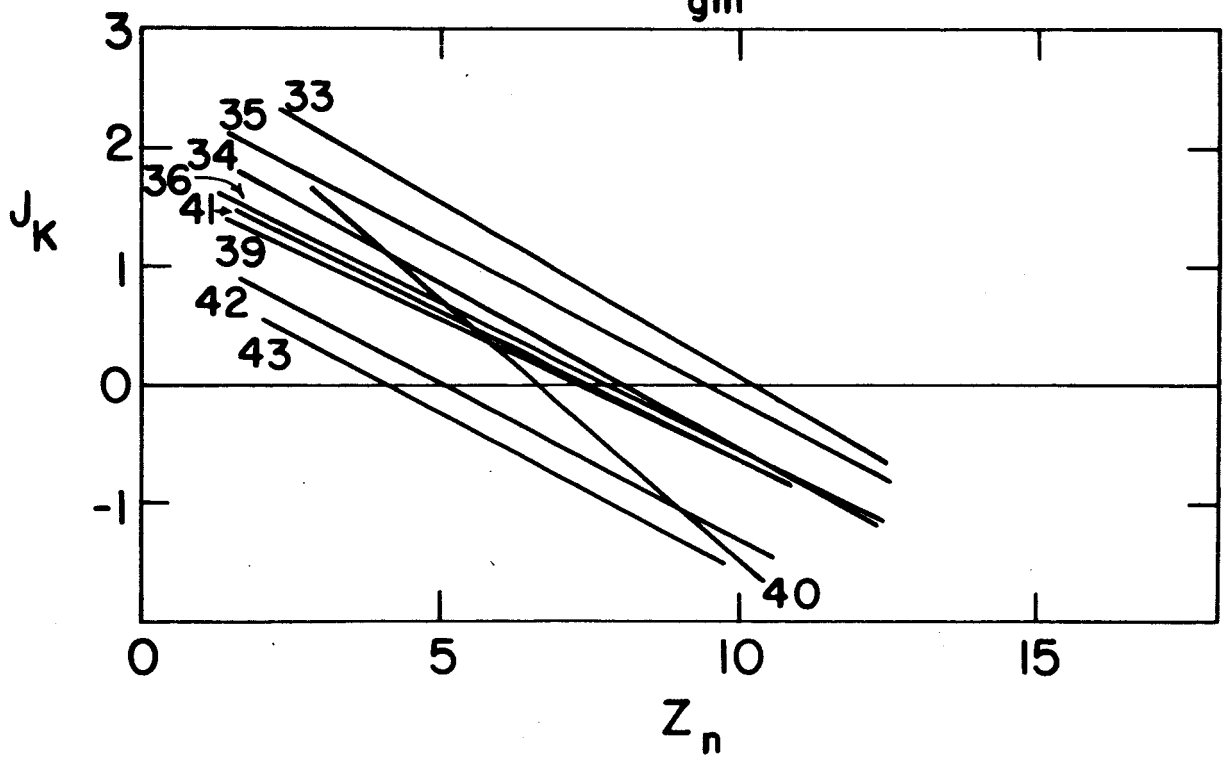
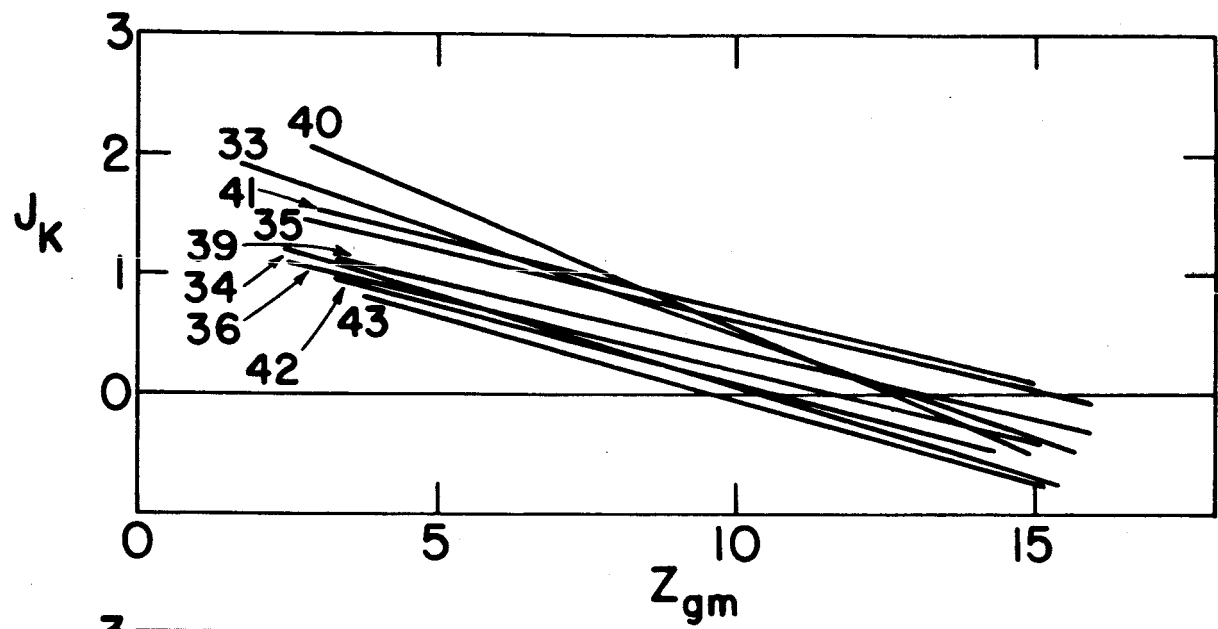


Fig.9

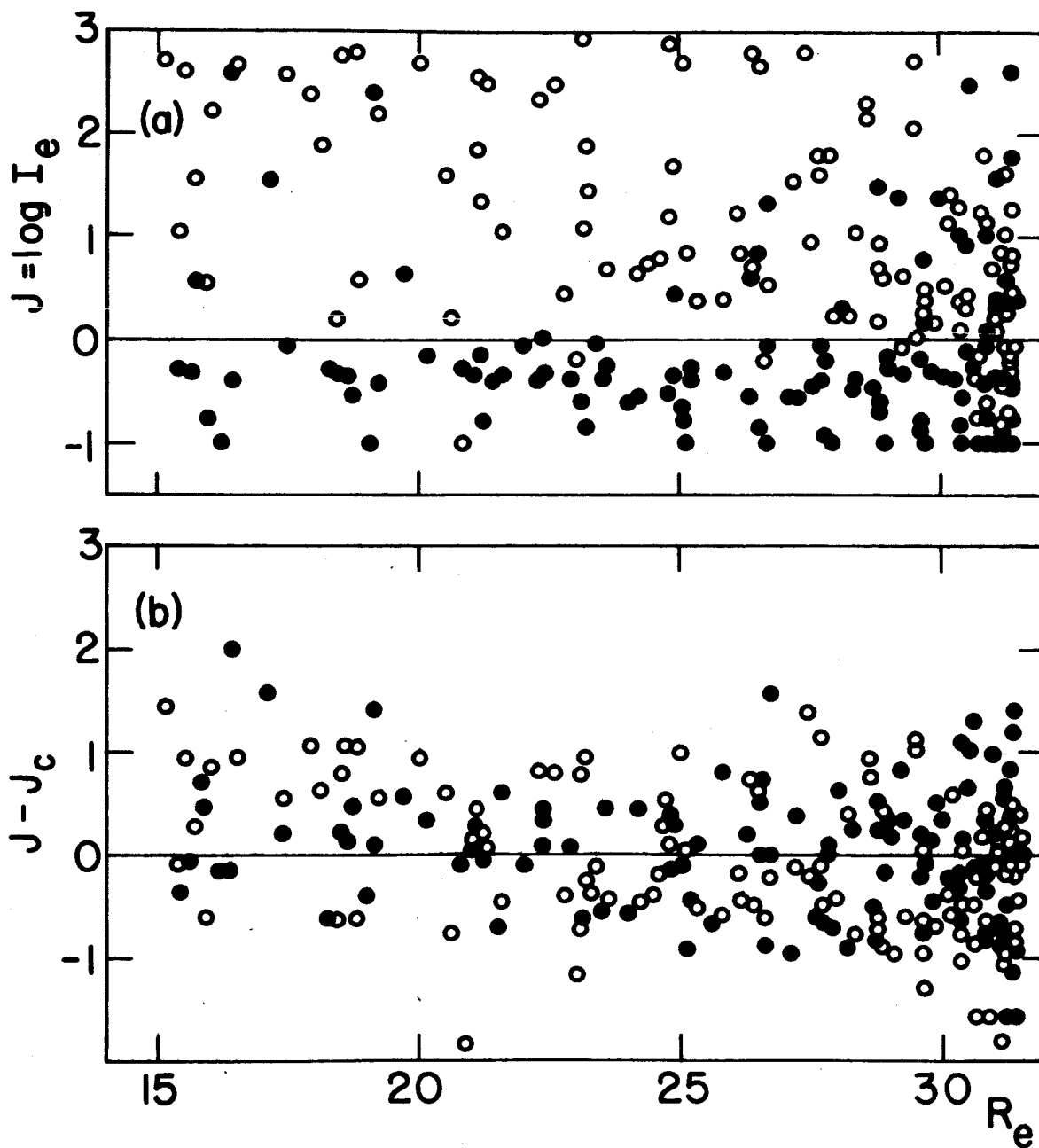


Fig.10

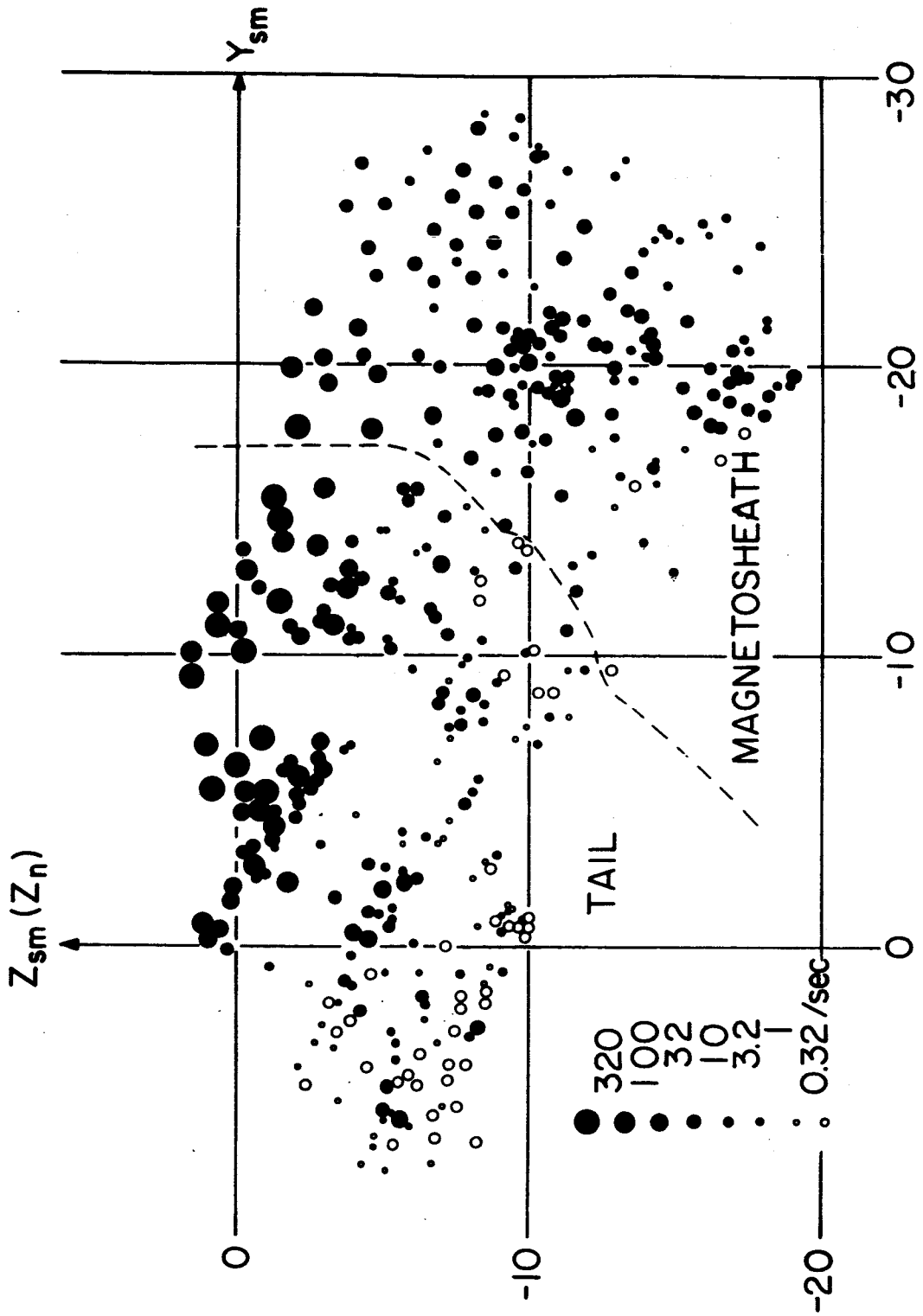


Fig. 11